

INSTITUTO
DE FÍSICA

preprint

IFUSP/P-102

CONTRIBUTION TO THE HEAVY-ION OPTICAL POTENTIAL
FROM COUPLING TO VIBRATIONAL STATES

by

R. Donangelo and L.F. Canto

Instituto de Física - Univ. Fed. do Rio de Janeiro

and

M.S. Hussein

Instituto de Física - Universidade de São Paulo

B.I.F. - USP

UNIVERSIDADE DE SÃO PAULO
INSTITUTO DE FÍSICA
Caixa Postal - 20.516
Cidade Universitária
São Paulo - BRASIL

IFUSP/P 102
B.I.F. - USP

CONTRIBUTION TO THE HEAVY-ION OPTICAL
POTENTIAL FROM COUPLING TO VIBRATIONAL STATES*

R. Donangelo and L.F.Canto

Instituto de Física da Universidade Federal do Rio de Janeiro -
20.000 - Rio de Janeiro - R.J. - Brasil

and

Mahir S. Hussein

Instituto de Física da Universidade de São Paulo, C.P. 20.516 -
01000 - São Paulo, S.P. Brasil

ABSTRACT

The component of the optical potential in the elastic channel due to the coupling to vibrational states in Coulomb excitation is derived using a previously developed semiclassical method. Several numerical examples are worked out.

* Supported in part by FINEP and CNPq.

1) INTRODUCTION

Most investigations of heavy-ion optical potentials have concentrated on calculating the real part of the potential. Recently there has been an upsurge of interest in calculating the imaginary part of the optical potential based on simple physical models. Love et al¹⁾ and Baltz et al²⁾ have applied Feshbach formalism³⁾ to calculate the absorptive potential in the elastic channel for the case of Coulomb excitation. In their calculation the potential was expanded in a perturbation series which was carried out to the lowest non trivial term. This implies that only the coupling to the first excited state is considered, and that multistep processes, such as those taking place in multiple Coulomb excitation, were not included in the calculation. It is however well known that multiple Coulomb excitation is frequently important in heavy-ion collisions. On the other hand, the difficulty in evaluating higher order terms in the perturbation expansion makes impractical the application of Feshbach theory to such strong coupling cases.

More recently an alternative approach has been proposed^{4),5),6)} on the basis of classical trajectories for the colliding nuclei, and subsequently applied to the case of Coulomb excitation of strongly deformed nuclei⁴⁾. This semiclassical approach has the advantage of including multistep processes in a natural way.

It was shown that in the small coupling limit this semiclassical theory yields the same potential as that of Baltz et al²⁾. In view of this we found interesting to apply this approach to other cases. In the present paper we use this semiclassical method to calculate the effective potential in the elastic channel associated with the coupling to vibrational

excitation of spherical nuclei.

In section 2 we give a short review of the method developed in our previous paper⁴⁾. In section 3 it is applied to calculate the optical potential due to vibrational coupling in spherical nuclei. Numerical results for several systems are presented in section 4. In section 5 we make some concluding remarks.

2) SEMICLASSICAL THEORY FOR EFFECTIVE LOCAL POTENTIAL

In a previous paper⁴⁾ it was shown that the contribution to the optical potential in the elastic channel from a given set of inelastic channels can be related to the elastic channel amplitudes by the expression

$$\bar{U}_l(r) = \frac{\hbar}{2} \left| \frac{dr_l}{dt} \right| \left\{ \frac{d}{dr} [\ln a_l^+(r)] - \frac{d}{dr} [\ln a_l^-(r)] \right\} \quad (1)$$

Here $a_l^\pm(r)$ are the elastic channel amplitudes evaluated at a separation r for the ingoing (-) and outgoing (+) branches of a classical trajectory with angular momentum number l .

For a Rutherford trajectory the quantity $\left| \frac{dr_l}{dt} \right|$ is given by

$$\left| \frac{dr_l}{dt} \right| = \left[\frac{2}{m} \left(E - \frac{Z_1 Z_2 e^2}{r} - \frac{\hbar^2 l^2}{2mr^2} \right) \right]^{1/2} \quad (2)$$

where E is the total energy in the center of mass frame of reference, m the reduced mass of the system, Z_1, Z_2 the atomic numbers of the colliding nuclei.

The physical implications of eq.(1) are easy to see. Since the effect of the optical potential is to change the elastic channel amplitude, by considering these changes at a given separation r , information about the effective potential at r is obtained. Both the ingoing and outgoing amplitudes appear in the expression since for each distance r the potential affects the amplitude twice: in the incoming and outgoing branches of the trajectory.

In ref.(4) the effective local potential $\bar{U}_l(r)$ was

evaluated for the case of Coulomb excitation of rotational states, and the results in the small coupling limit were shown to coincide with the potential derived by Baltz et. al²⁾.

3) EFFECTIVE LOCAL POTENTIAL FOR VIBRATIONS

The theory presented in the previous section may be applied to the case where the inelastic channels that affect the elastic scattering process correspond to collective nuclear vibrations.

At energies below that of the Coulomb barrier, where the nuclear forces between target and projectile nuclei are not felt, the amplitudes appearing in Eq.(1) may be evaluated using the semiclassical theory of Alder and Winther⁷⁾. When applied to the particular case of vibrational excitation this theory has the advantage that the excitation amplitudes are given in closed form.

Let us consider a situation where the elastic channel $|0,00\rangle$ is coupled to vibrational states $|n, \lambda, \mu\rangle$ consisting of n phonons of a given multipolarity λ, μ . The generalization to simultaneously include phonons of different multiplicities in the present formalism is straight-forward. The amplitude in the elastic channel is given by⁷⁾

$$a_l^{\lambda, \mu}(t) = \exp\left[-\frac{1}{2} \left| \chi^{(\lambda)} a_{\lambda-\mu}(\theta, \frac{t}{v}, t) \right|^2\right] \quad (3)$$

where the strength parameter $\chi^{(\lambda)}$ is defined as⁷⁾

$$\chi^{(\lambda)} = \frac{\sqrt{16\pi} (\lambda-1)!}{(2\lambda+1)!!} \frac{E_1 e^{-i\pi/2}}{\hbar v} \frac{[B(E\lambda, I_1 \rightarrow I_2)]^2}{\lambda} \quad (4)$$

in terms of the projectile atomic number, Z_1 , the reduced transition probability $B(E\lambda, I_1 \rightarrow I_2)$, the asymptotic

relative velocity v and the half distance of closest approach for head-on collision a . The orbital integral $R_{\lambda-\mu}(\theta, \xi, t)$ appearing in the exponent of Eq. (3) can be expressed in terms of the Rutherford trajectory $r(t), \varphi(t)$ as

$$R_{\lambda-\mu}(\theta, \xi, t) = \frac{v^{-\lambda} a^{\lambda} (2\lambda-1)!!}{(\lambda-1)!!} \left[\frac{\pi}{2\lambda+1} Y_{\lambda-\mu}\left(\frac{\pi}{2}, \nu\right) \right]^{\lambda} \times \int_{-a}^t \frac{\exp[-i\mu\varphi(t) + i\xi(v/a)t]}{[r(t)]^{\lambda+1}} dt \quad (5)$$

where ξ is the adiabaticity parameter, as defined in ref. (3).

Inserting Eq. (3) into Eq. (1) we obtain

$$\bar{U}_{\lambda}^{(\lambda, \mu)}(r) = -\frac{i\hbar}{4} |\chi^{(\lambda)}|^2 \left\{ \frac{d}{dt} \left| R_{\lambda-\mu}(\theta, \xi, t_{\lambda}^{+}(r)) \right|^2 + \frac{d}{dt} \left| R_{\lambda-\mu}(\theta, \xi, t_{\lambda}^{-}(r)) \right|^2 \right\} \quad (6)$$

where $t_{\lambda}^{+}(r)$ ($t_{\lambda}^{-}(r)$) are the times at which the distance between projectile and target centers equals r , on the outgoing (incoming) branches of the Rutherford trajectory. Now taking to be zero the time at the distance of closest approach, and defining

$$t_{\lambda}^{+}(r) = -t_{\lambda}^{-}(r) \equiv t_{\lambda}(r) \quad (7)$$

we obtain after substituting (5) into (6)

$$\bar{U}_{\lambda}^{(\lambda, \mu)}(r) = -\frac{i\hbar}{4} |\chi^{(\lambda)}|^2 \frac{2\pi}{2\lambda+1} \left[\frac{v^{-\lambda} a^{\lambda} (2\lambda-1)!!}{(\lambda-1)!!} Y_{\lambda-\mu}\left(\frac{\pi}{2}, \nu\right) \right]^2 \times \frac{1}{[r]^{\lambda+1}} \frac{1}{v^{-\lambda} a^{\lambda}} \cos \left[\mu\varphi(t) - \xi \frac{v t_{\lambda}(r)}{a} \right]^{\lambda} \times I_{\lambda-\mu}(\theta, \xi) \quad (8)$$

where $I_{\lambda-\mu}(\theta, \xi)$ is the usual Coulomb excitation function, as defined in Appendix H of Ref. (7) and whose numerical values are found in Ref. (8). In the sudden limit ($\dot{\gamma} = 0$), $I_{\lambda-\mu}$ may be expressed in terms of elementary functions. The deflection angle θ is related to the orbital angular momentum l through the relation

$$\frac{l}{\eta} = \cot \frac{\theta}{2} \quad (9)$$

in which $\eta = Z_1 Z_2 e^2 / h v$ is the Sommerfeld parameter.

The total effective optical potential is obtained by summing over all vibrational modes

$$\bar{U}_l(r) = \sum_{\lambda, \mu} \bar{U}_{\lambda, \mu}^{(l)}(r) \quad (10)$$

In the case of spherical nuclei the strength of each term appearing in eq. (10) depends essentially on λ . The effective optical potential associated with each multipolarity λ may then be obtained by summing over the corresponding values of μ . For the frequently dominant modes $\lambda = 2$ and $\lambda = 3$ the results are

$$\bar{U}_l^{(\lambda=2)}(r) = - \frac{9}{64} i \hbar \frac{v^{-1} a^2 |\alpha^{(2)}|^2}{r^3} \cos \left[\frac{\xi v t_p(r)}{a} \right] \times \quad (11)$$

$$\times \left[2 I_{20}(\theta, \xi) + 3 \cos^2 \alpha \varphi_2(r) \left(I_{22}(\theta, \xi) + I_{2-2}(\theta, \xi) \right) \right]$$

$$\bar{U}_l^{(\lambda=3)}(r) = - \frac{225}{512} i \hbar \frac{v^{-1} a^3 |\alpha^{(3)}|^3}{r^4} \cos \left[\frac{\xi v t_p(r)}{a} \right] \times \quad (12)$$

$$\times \left[3 \cos \alpha \varphi_3(r) \left(I_{31}(\theta, \xi) + I_{3-1}(\theta, \xi) \right) + \right.$$

$$\left. + 5 \cos^3 \alpha \varphi_3(r) \left(I_{33}(\theta, \xi) + I_{3-3}(\theta, \xi) \right) \right]$$

In the $\xi = 0$ limit eq. (11) reduces to

$$\begin{aligned} \bar{U}_\lambda^{\lambda=2}(r) = & -\frac{q}{32} i \hbar \frac{v^{-\alpha} |\chi^{(2)}|^2}{r^3} \left[\frac{\eta^4 (3\ell^2 + \eta^2)}{\ell^2 (\ell^2 + \eta^2)} - \right. \\ & - \frac{\eta^3}{\ell^3} \operatorname{Arctan} \left(\frac{\ell}{\eta} \right) + \frac{\eta^2 \ell^2}{(\ell^2 + \eta^2)^2} \left(\frac{\alpha}{r} \right) \\ & \left. + \frac{2\ell^4}{(\ell^2 + \eta^2)^2} \left(\frac{\alpha^2}{r} \right) \right] \quad (13) \end{aligned}$$

where use has been made of the relation

$$\cos \varphi(r) = \frac{1 + \frac{\ell^2}{\eta^2} \left(\frac{\alpha}{r} \right)}{\sqrt{1 + \frac{\ell^2}{\eta^2}}} \quad (14)$$

as well as of the analytical expressions for $I_{20}(\theta, \omega)$, $I_{22}(\theta, \omega)$ ⁷⁾ written in terms of λ through use of eq. (9).

The expression found for the effective potential (eq. (13)) is exactly the same as that for the rotational case in the same $\xi = 0$ limit. This is a remarkable fact since the latter was lowest order approximation, valid only for small values of the coupling parameter $\chi^{(2)}$, whereas (13) is exact, aside from the semiclassical assumptions implicit in its derivation. The quadratic $\chi^{(2)}$ -dependance of the potential $\bar{U}_\lambda^{\lambda}(r)$ is a direct consequence of the pure harmonic nature of the vibrational states considered. The deviations from this quadratic behaviour in the case of rotations, which in ref. (4) were shown to be important for large values of the quadrupole coupling parameter q_2

$$q_2 = \sqrt{\frac{45}{16}} \chi^{(2)} \quad (15)$$

are due to anharmonicities arising from phonon-phonon interac-

tions. These anharmonic effects appear in the description of vibrational nuclei, but they become much more important for rotational states. In this case they are predominant so that the potential given by (13) is no longer valid and the more complex potential presented in Ref. (4) has to be used.

4) NUMERICAL RESULTS

As an example we show in fig. (9) the effective potential for the scattering of ^{40}Ar off the vibrational nucleus ^{194}Pt at an energy around the Coulomb barrier. The λ value of the partial wave corresponding to the grazing angle is about 175. The results are given both for the $\xi \neq 0$ case of eq.(11) as well as for the sudden limit considered in eq.(13). One readily notices that the ratio $[\overline{U}_\lambda(r) (\xi \neq 0)] / [\overline{U}_\lambda(r) (\xi = 0)]$ is not the simple constant $g_2(\xi)$ as it is suggested for the case of rotational excitation in ref. (2), but depends both on the angular momentum λ and the radial separation r . We should remark that although eqs.(11) and (13) were derived for values of r on Rutherford trajectories the expression for the potential is also valid inside the classically forbidden region, i.e. for $r < r_{min}$ where

$$\frac{Z_1 Z_2 e^2}{r_{min}} + \frac{\hbar^2 \lambda^2}{2 M r_{min}^2} = E \quad (16)$$

This corresponds to assuming complex values for the time inside the classically forbidden region⁹⁾. To illustrate the effect of this potential we show in fig.(2) the changes induced by this potential on the simple sharp cut-off elastic cross section¹⁰⁾. In this case the calculations done with the potentials for $\xi \neq 0$ and $\xi = 0$ show no appreciable difference and would lie on top of each other in the figure. This indicates that at least for values of $\xi \lesssim 0.2$ the simpler expression (13) is quite adequate.

In Table I we present values of the potential $\overline{U}_\lambda(r)$ for several physical systems, calculated using eq.(11) and in the sudden limit given by eq.(13). The values of $\beta(E2) \uparrow$ and

E_{2^+} used to evaluate $\chi^{(2)}$ and ξ were taken from Nuclear Data Sheets and the value of the angular momentum L_{grazing} was estimated from the expression

$$L_g = 1.2 (A_1^{1/3} + A_2^{1/3}) k \quad (17)$$

where A_1 and A_2 are the mass numbers of the colliding nuclei and k is the asymptotic wave number of the relative motion

$$k = \frac{mv}{\hbar} = \frac{\eta}{a} \quad (18)$$

The deflection angles θ_{grazing} at which σ/σ_R were evaluated are related to L_{grazing} through eq.(9). The values of σ/σ_R shown in the table should be compared to the value

$\sigma/\sigma_R = 0.25$ obtained in the absence of the absorptive potential $\bar{U}_l(r)$. We notice that although the magnitude of the potential $\bar{U}_l(r_{\text{min}})$ is no more than a few tenths of an MeV, even in the case of very heavy systems, its overall effect on the cross section can be appreciable (see fig.2), due to its long-range character.

5) CONCLUDING REMARKS

In this work the semiclassical method developed in ref. 4) was used to calculate the contribution to the optical potential in the elastic channel due to the coupling to vibrational states in spherical nuclei. Explicit formulae for the effective potential in the case of quadrupole and octupole harmonic vibrations were derived. It was shown that in the sudden limit ($\xi=0$) the exact (aside from semiclassical approximations) potential for quadrupole vibrations is identical to the potential of Baltz et al.²⁾ It should be clear that these potentials would differ either if anharmonicities were included in the description of the vibrations or if multistep processes were considered in Baltz's calculation. It was also shown that the ξ -dependence of the potential does not have the simple character of a factor $g_2(\xi)$ multiplying the $\xi=0$ potential.²⁾ The ratio $[\bar{U}_\lambda(r), \xi \neq 0] / [\bar{U}_\lambda(r), \xi = 0]$ was shown to depend both on γ and λ . On the other hand a test calculation revealed that for $\xi \lesssim 0.2$ the cross sections obtained with the use of the effective potential do not change appreciably with ξ . Thus one may confidently use the simpler $\xi=0$ expressions for the potential, at least for these low ξ values.

It is interesting to note that in spite of these effective potentials being derived through the use of classical trajectories, their validity is not restricted to the classically accessible region. By considering complex Rutherford trajectories it may be shown that the expressions in the classical region can be analytically extended to the forbidden region.

Further applications of this semiclassical method are being considered.

REFERENCES

- 1) W.G.Low, T.Terasawa and G.R.Satchler - Phys.Rev.Lett. 39 6 (1977).
- 2) A.J.Baltz, S.K.Kauffmann, N.K.Glendenning and K.Pruess - Phys.Rev.Lett. 40, 20 (1978).
- 3) H.Feshbach - Ann.Phys. (N.Y.) 19, 287 (1962).
- 4) R.Donangelo, L.F.Canto and M.S.Hussein - IFUSP Preprint 152 (1978) submitted to Nuclear Physics A.
- 5) Aa. Winther - private communication.
- 6) D.M.Brink - private communication.
- 7) K.Alder and Aa.Winther - "Electromagnetic Excitations" (Noth-Holland-American Elsevier) (1975)
- 8) K.Alder and Aa.Winther, Mat.Fys.Medd.Dan.Vid.Selck. 31, n^o 1 (1956).
- 9) W.H.Miller - Adv.Chem.Phys. 25, 69 (1974).
- 10) W.E.Frahn, in "Heavy-ion, High Spin States and Nuclear Structure" Vol.I p.157, International Atomic Energy Agency, Vienna, 1975.

TABLE CAPTIONS

TABLE I - Strengths of the absorptive potentials and values of σ/σ_r at the grazing angle for several systems. The potentials shown were evaluated for the grazing angular momentum at the distance of closest approach γ_{\min} (eq.16). The laboratory energies indicated correspond to the respective Coulomb barrier heights for these systems.

FIGURE CAPTIONS

FIG.1 - The long-range component of the elastic channel optical potential for the system $^{40}\text{Ar} + ^{194}\text{Pt}$. The full line corresponds to eq.(11) in the text whereas the dashed line refers to eq.(13). The abscissa is the radial separation measured in units of a (see text).

FIG.2 - The elastic cross-section for $^{40}\text{Ar} + ^{194}\text{Pt}$, normalized to the Rutherford cross-section, both with and without the absorptive potential of fig.1. Other parameters used in this calculation are shown in Table I.

SYSTEM	E_{Lab} (MeV)	η	a (fm)	$\alpha^{(2)}$	L_g	$\bar{U}_{Lg} (r_{\text{min}})$ (MeV)		σ/σ_R (θ grazing)
						$\xi \neq 0$	$\xi = 0$	
$^{16}\text{O} + ^{76}\text{Ge}$	47	23.5	4.7	0.9	40	0.017	0.022	0.23
$^{16}\text{O} + ^{110}\text{Pd}$	59	30.1	5.1	1.2	52	0.037	0.038	0.22
$^{16}\text{O} + ^{194}\text{Pt}$	84	43.0	5.8	1.0	74	0.029	0.029	0.23
$^{40}\text{Ar} + ^{76}\text{Ge}$	118	52.8	5.4	1.6	90	0.053	0.059	0.21
$^{40}\text{Ar} + ^{110}\text{Pd}$	141	69.3	5.7	2.2	119	0.11	0.11	0.17
$^{40}\text{Ar} + ^{194}\text{Pt}$	189	102.	6.4	1.9	174	0.091	0.095	0.18
$^{132}\text{Xe} + ^{194}\text{Pt}$	669	295	7.6	4.0	505	0.34	0.036	0.063

TABLE I

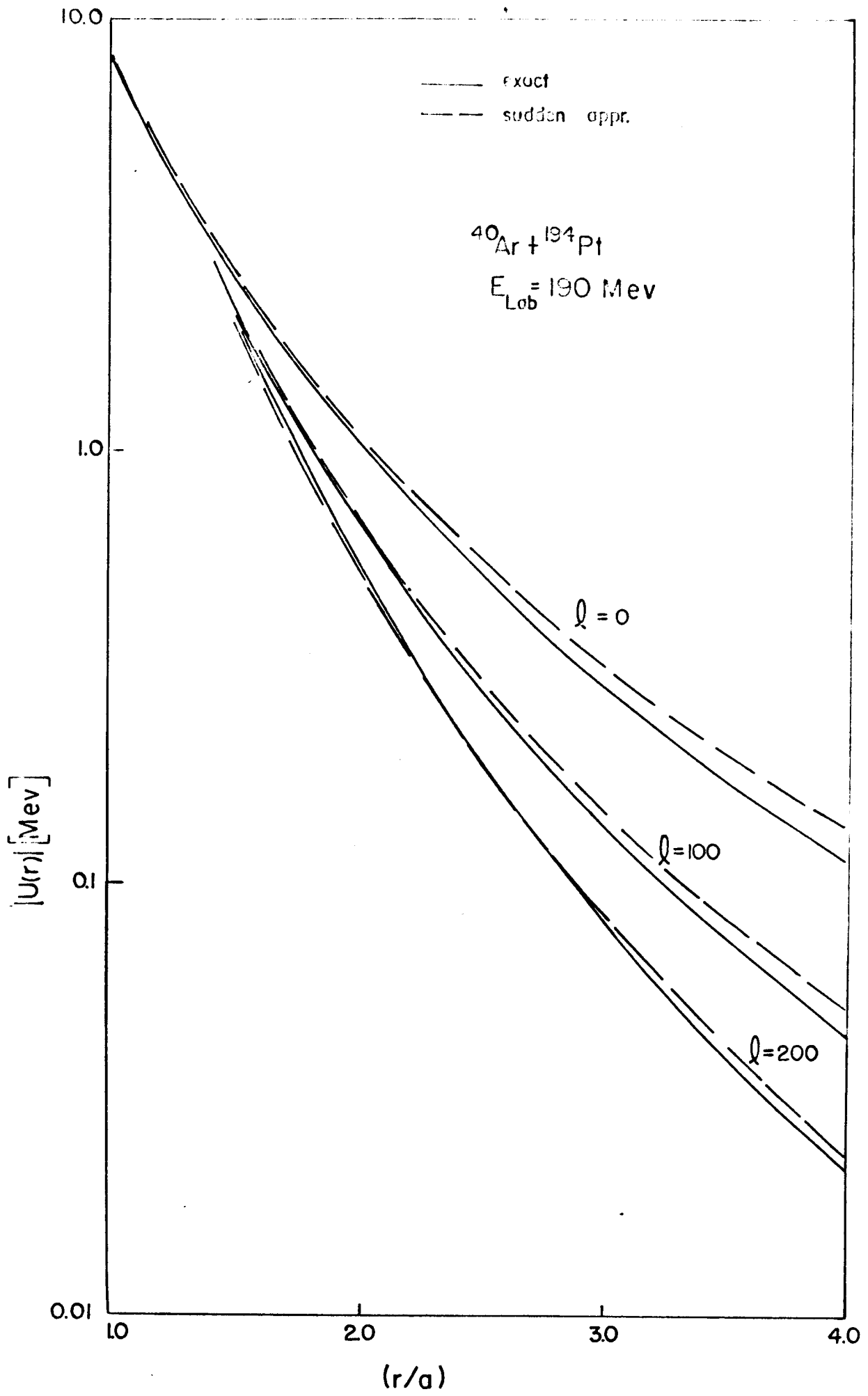


FIG.1

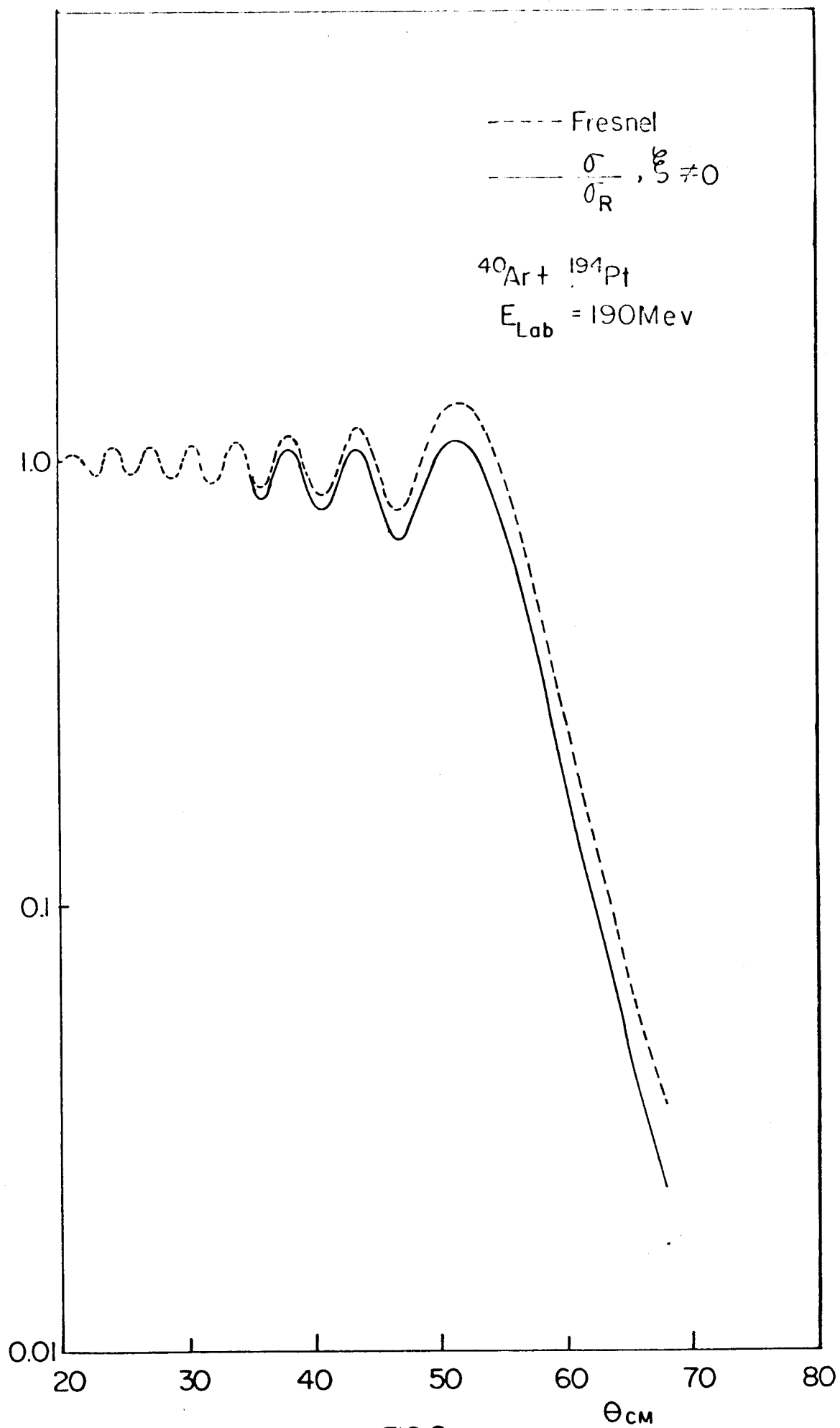


FIG. 2